

## New measurement of the $^{242}\text{Pu}(n,\gamma)$ cross section at n\_TOF-EAR1 for MOX fuels: Preliminary results in the RRR

J. Leredegui-Marco<sup>1,a</sup>, C. Guerrero<sup>1</sup>, M.A. Cortés-Giraldo<sup>1</sup>, J.M. Quesada<sup>1</sup>, E. Mendoza<sup>2</sup>, D. Cano-Ott<sup>2</sup>, K. Eberhardt<sup>3</sup>, A. Junghans<sup>4</sup>, O. Aberle<sup>5</sup>, J. Andrzejewski<sup>6</sup>, L. Audouin<sup>7</sup>, M. Bacak<sup>8,5,9</sup>, J. Balibrea<sup>6</sup>, M. Barbagallo<sup>10</sup>, F. Bečvář<sup>11</sup>, E. Berthoumieux<sup>9</sup>, J. Billowes<sup>12</sup>, D. Bosnar<sup>13</sup>, A. Brown<sup>14</sup>, M. Caamaño<sup>15</sup>, F. Calviño<sup>16</sup>, M. Calviani<sup>5</sup>, R. Cardella<sup>5</sup>, A. Casanovas<sup>16</sup>, F. Cerutti<sup>5</sup>, Y.H. Chen<sup>7</sup>, E. Chiaveri<sup>5,12,14</sup>, N. Colonna<sup>10</sup>, G. Cortés<sup>16</sup>, L. Cosentino<sup>17</sup>, L.A. Damone<sup>10,18</sup>, M. Diakaki<sup>9</sup>, C. Domingo-Pardo<sup>19</sup>, R. Dressler<sup>20</sup>, E. Dupont<sup>9</sup>, I. Durán<sup>15</sup>, B. Fernández-Domínguez<sup>15</sup>, A. Ferrari<sup>5</sup>, P. Ferreira<sup>21</sup>, P. Finocchiaro<sup>17</sup>, K. Göbel<sup>22</sup>, M.B. Gómez-Hornillos<sup>16</sup>, A.R. García<sup>6</sup>, A. Gawlik<sup>6</sup>, S. Gilardoni<sup>5</sup>, T. Glodariu<sup>23</sup>, I.F. Gonçalves<sup>21</sup>, E. González<sup>6</sup>, E. Griesmayer<sup>8</sup>, F. Gunsing<sup>9,5</sup>, H. Harada<sup>24</sup>, S. Heinitz<sup>20</sup>, J. Heyse<sup>25</sup>, D.G. Jenkins<sup>14</sup>, E. Jericha<sup>8</sup>, F. Käppler<sup>26</sup>, Y. Kadi<sup>5</sup>, A. Kalamara<sup>27</sup>, P. Kavargin<sup>8</sup>, A. Kimura<sup>24</sup>, N. Kivel<sup>20</sup>, M. Kokkoris<sup>27</sup>, M. Krtička<sup>11</sup>, D. Kurtulgi<sup>22</sup>, E. Leal-Cidoncha<sup>15</sup>, C. Lederer<sup>28</sup>, H. Leeb<sup>8</sup>, S. Lo Meo<sup>29,30</sup>, S.J. Lonsdale<sup>28</sup>, D. Macina<sup>5</sup>, J. Marganiec<sup>6,31</sup>, T. Martínez<sup>6</sup>, A. Masi<sup>5</sup>, C. Massimi<sup>30,32</sup>, P. Mastinu<sup>33</sup>, M. Mastromarco<sup>10</sup>, E.A. Mauger<sup>20</sup>, A. Mazzone<sup>10,34</sup>, A. Mengoni<sup>29</sup>, P.M. Milazzo<sup>35</sup>, F. Mingrone<sup>5</sup>, A. Musumarra<sup>17,36</sup>, A. Negret<sup>23</sup>, R. Nolte<sup>31</sup>, A. Oprea<sup>23</sup>, N. Patronis<sup>37</sup>, A. Pavlik<sup>38</sup>, J. Perkowski<sup>6</sup>, I. Porras<sup>39</sup>, J. Praena<sup>39</sup>, D. Radeck<sup>31</sup>, T. Rauscher<sup>40,41</sup>, R. Reifarh<sup>22</sup>, P.C. Rout<sup>42</sup>, C. Rubbia<sup>5</sup>, J.A. Ryan<sup>12</sup>, M. Sabaté-Gilarte<sup>5,14</sup>, A. Saxena<sup>42</sup>, P. Schillebeeckx<sup>25</sup>, D. Schumann<sup>20</sup>, A.G. Smith<sup>12</sup>, N.V. Sosnin<sup>12</sup>, A. Stamatopoulos<sup>27</sup>, G. Tagliente<sup>10</sup>, J.L. Tain<sup>19</sup>, A. Tarifeño-Saldivia<sup>16</sup>, L. Tassan-Got<sup>7</sup>, S. Valenta<sup>11</sup>, G. Vannini<sup>30,32</sup>, V. Variale<sup>10</sup>, P. Vaz<sup>21</sup>, A. Ventura<sup>30</sup>, V. Vlachoudis<sup>5</sup>, R. Vlastou<sup>27</sup>, A. Wallner<sup>43</sup>, S. Warren<sup>12</sup>, P.J. Woods<sup>28</sup>, T. Wright<sup>12</sup>, P. Žugec<sup>13,5</sup>, and the n\_TOF Collaboration

<sup>1</sup> Universidad de Sevilla, Spain

<sup>2</sup> Centro de Investigaciones Energeticas Medioambientales y Tecnológicas (CIEMAT), Spain

<sup>3</sup> Johannes Gutenberg-Universität Mainz, 55128 Mainz, Germany

<sup>4</sup> Helmholtz-Zentrum Dresden-Rossendorf, 01314 Dresden, Germany

<sup>5</sup> European Organization for Nuclear Research (CERN), Switzerland

<sup>6</sup> University of Lodz, Poland

<sup>7</sup> Institut de Physique Nucléaire, CNRS-IN2P3, Univ. Paris-Sud, Université Paris-Saclay, 91406 Orsay Cedex, France

<sup>8</sup> Technische Universität Wien, Austria

<sup>9</sup> CEA Saclay, Irfu, Gif-sur-Yvette, France

<sup>10</sup> Istituto Nazionale di Fisica Nucleare, Sezione di Bari, Italy

<sup>11</sup> Charles University, Prague, Czech Republic

<sup>12</sup> University of Manchester, UK

<sup>13</sup> University of Zagreb, Croatia

<sup>14</sup> University of York, UK

<sup>15</sup> University of Santiago de Compostela, Spain

<sup>16</sup> Universitat Politècnica de Catalunya, Spain

<sup>17</sup> INFN Laboratori Nazionali del Sud, Catania, Italy

<sup>18</sup> Dipartimento di Fisica, Università degli Studi di Bari, Italy

<sup>19</sup> Instituto de Física Corpuscular, Universidad de Valencia, Spain

<sup>20</sup> Paul Scherrer Institut (PSI), Villingen, Switzerland

<sup>21</sup> Instituto Superior Técnico, Lisbon, Portugal

<sup>22</sup> Goethe University Frankfurt, Germany

<sup>23</sup> Horia Hulubei National Institute of Physics and Nuclear Engineering, Romania

<sup>24</sup> Japan Atomic Energy Agency (JAEA), Tokai-mura, Japan

<sup>25</sup> European Commission, Joint Research Centre, Geel, Retieseweg 111, 2440 Geel, Belgium

<sup>26</sup> Karlsruhe Institute of Technology, Campus North, IKP, 76021 Karlsruhe, Germany

<sup>27</sup> National Technical University of Athens, Greece

<sup>28</sup> School of Physics and Astronomy, University of Edinburgh, UK

<sup>29</sup> Agenzia nazionale per le nuove tecnologie (ENEA), Bologna, Italy

<sup>30</sup> Istituto Nazionale di Fisica Nucleare, Sezione di Bologna, Italy

<sup>31</sup> Physikalisch-Technische Bundesanstalt (PTB), Bundesallee 100, 38116 Braunschweig, Germany

<sup>32</sup> Dipartimento di Fisica e Astronomia, Università di Bologna, Italy

<sup>a</sup>e-mail: jlerendegui@us.es

- <sup>33</sup> Istituto Nazionale di Fisica Nucleare, Sezione di Legnaro, Italy
- <sup>34</sup> Consiglio Nazionale delle Ricerche, Bari, Italy
- <sup>35</sup> Istituto Nazionale di Fisica Nucleare, Sezione di Trieste, Italy
- <sup>36</sup> Dipartimento di Fisica e Astronomia, Università di Catania, Italy
- <sup>37</sup> University of Ioannina, Greece
- <sup>38</sup> University of Vienna, Faculty of Physics, Vienna, Austria
- <sup>39</sup> University of Granada, Spain
- <sup>40</sup> Department of Physics, University of Basel, Switzerland
- <sup>41</sup> Centre for Astrophysics Research, University of Hertfordshire, UK
- <sup>42</sup> Bhabha Atomic Research Centre (BARC), India
- <sup>43</sup> Australian National University, Canberra, Australia

**Abstract.** The spent fuel of current nuclear reactors contains fissile plutonium isotopes that can be combined with  $^{238}\text{U}$  to make mixed oxide (MOX) fuel. In this way the Pu from spent fuel is used in a new reactor cycle, contributing to the long-term sustainability of nuclear energy. The use of MOX fuels in thermal and fast reactors requires accurate capture and fission cross sections. For the particular case of  $^{242}\text{Pu}$ , the previous neutron capture cross section measurements were made in the 70's, providing an uncertainty of about 35% in the keV region. In this context, the Nuclear Energy Agency recommends in its "High Priority Request List" and its report WPEC-26 that the capture cross section of  $^{242}\text{Pu}$  should be measured with an accuracy of at least 7–12% in the neutron energy range between 500 eV and 500 keV. This work presents a brief description of the measurement performed at n\_TOF-EAR1, the data reduction process and the first ToF capture measurement on this isotope in the last 40 years, providing preliminary individual resonance parameters beyond the current energy limits in the evaluations, as well as a preliminary set of average resonance parameters.

## 1. Introduction and motivation

The measurement of accurate capture and fission cross sections is essential for the design and operation of innovative nuclear systems aimed at the reduction of the nuclear waste [1]. The spent fuel from current nuclear reactors contains a significant fraction of plutonium, which can be separated from the fuel matrix and combined with depleted uranium ( $^{238}\text{U}$ ) to make what is known as mixed oxide (MOX) fuel [2], contributing therefore to the long-term sustainability of nuclear energy. Currently, the use of MOX fuel in thermal power reactors has been established in several countries. However, a much more efficient use of plutonium will ultimately be made in fast reactors, where multiple recycling is possible and has been demonstrated [2]. The extensive use of MOX fuels in fast reactors calls for a revision of the neutron cross sections that play a role in the neutronics of such reactors and are not known with enough accuracy yet. For the particular case of  $^{242}\text{Pu}$ , both the uncertainties in the experimental data and the discrepancies in the average resonance parameters between the optical model calculations and the statistical analysis of s-wave resonances, call for a new measurement of the capture cross section. The reader is referred to Ref. [3] for a more detailed description of the motivations.

Following the suggestion of the NEA in its High Priority Request List [4], a new measurement of the  $^{242}\text{Pu}$  cross section at the n\_TOF facility was proposed and approved by the CERN ISOLDE and Neutron Time-of-Flight Committee (INTC) [5] and the experiment was successfully performed in summer 2015. In the following section we briefly describe the n\_TOF facility, the experimental setup and the  $^{242}\text{Pu}$  target and in Sect. 3 the main features of the measuring technique and the steps involved in the data reduction process. Last, the preliminary analysis in the Resolved Resonance Region (RRR) is presented in Sect. 4.

## 2. Measurement at n\_TOF-EAR1: Detectors and $^{242}\text{Pu}$ sample

The pulsed neutron beam at n\_TOF is generated through spallation of 20 GeV/c protons from the CERN Proton Synchrotron (CPS) impinging on a thick lead target. Each proton bunch contains, on average,  $7 \cdot 10^{12}$  protons with a time distribution of  $\sigma = 7$  ns and an average repetition rate of 0.17 Hz. The spallation neutrons, with energies in the MeV-GeV range, are partially moderated in the water cooling and moderation layers around the lead target and travel towards the experimental areas along two beam lines: EAR1 [6] at 185 m (horizontal) and EAR2 [7] at 19 m (vertical). The measurement presented in this work was performed in EAR1, featuring a better time resolution and consequently a better capability to resolve resonances up to higher neutron energies than in EAR2.

Neutrons coming from the spallation target, travel 185 m in vacuum along the beam line until they reach the  $^{242}\text{Pu}$  sample, with a diameter (45 mm) larger than the beam. The sample consisted on 95 mg of more than 99% pure  $^{242}\text{Pu}$  electrodeposited on a series of seven thin backings and was prepared within the CHANDA project [10] by the University of Mainz and the HZDR research center.

An array of four Total Energy detectors (BICRON) deuterized benzene ( $\text{C}_6\text{D}_6$ ) scintillators [8]) was used in this measurement. These detectors have been chosen for this measurement mainly because they suffer significantly less from the so-called  $\gamma$ -flash than the n\_TOF TAC [9], thus allowing us to measure up to the required neutron energy, and a much lower neutron sensitivity than the latter. More details on the experimental setup, sample preparation and data acquisition system are given in Ref. [3].

## 3. Data reduction

A detailed explanation of the data reduction process is out of the scope of this paper and in the following we just highlight the main steps of the analysis. First, the initially

measured quantities are counting rates as a function of time-of-flight (ToF). In order to reconstruct the neutron energy  $E_n$  (eV) the following non-relativistic time-to-energy relation is used

$$E_n = \left( 72.29 \frac{L_0 + \lambda(E_n)}{ToF} \right)^2,$$

where  $L_0$  (m) is the flight path from the target exit to the experimental,  $ToF$  is expressed in  $\mu s$  and  $\lambda(E_n)$  (m) is the time-of-flight resolution function, an energy-dependent equivalent moderation length in the target-moderator assembly that takes into account for the non-univocal relation between production time and neutron energy, obtained from the simulations of the n\_TOF spallation target [11].

Neutron capture measurements with  $C_6D_6$  detectors are analyzed following the Total Energy Detection Technique (TED) [12,13]. This technique is based on detecting just one  $\gamma$ -ray per cascade with an efficiency ( $\varepsilon_i$ ) proportional to its energy ( $E_i$ ), so that the overall efficiency for a capture cascade is, assuming ( $E_i$ ) sufficiently small,  $\varepsilon_c \propto \sum_i E_i \propto E_c$ , proportional to total cascade energy and independent of the actual cascade path.  $C_6D_6$  detectors in this setup feature low efficiencies ( $\sim 1\%$  for 1 MeV)  $\gamma$ -rays. However, they do not fulfill  $\varepsilon_i \propto E_i$ . Therefore, the Pulse Height Weighting Technique (PHWT) is used to weight each count with an energy (pulse height) factor so that this condition is fulfilled. This technique requires a good knowledge of the detector response to  $\gamma$ -rays in the energy range typical of capture cascades, i.e., up to 10 MeV. Monte Carlo simulations, performed in this work using the Geant4 toolkit [14], are the best solution. (See Ref. [3] for more details).

The total weighted counts include also several background components, that must be subtracted. These are determined with the help of several ancillary measurements, shown in Fig. 1: the dummy sample is a replica of the  $^{242}\text{Pu}$  assembly without  $^{242}\text{Pu}$  deposits inside and is causing the main neutron related background component. In addition, we also have to consider the beam-off background with and without the  $^{242}\text{Pu}$  targets in place. Last, the scattering in the target of in-beam  $\gamma$ -rays, produced along with neutrons in the spallation target, also contribute to the background, especially for targets with a high atomic number. The latter is estimated with help of a Pb target, featuring a high atomic number and a negligible capture cross section. The counting rate measured with the lead sample in place is scaled to the  $^{242}\text{Pu}$  sample according to the result of Geant4 simulations aimed at studying the background induced by in-beam  $\gamma$ -rays scattered in both, Pb and Pu, targets.

Last, to extract the neutron capture yield,

$$Y_{exp}(E_n) = \frac{f_c}{f_{SRM}} \cdot \frac{C_w(E_n) - B_w(E_n)}{\Phi(E_n) \cdot \varepsilon},$$

the background-subtracted counting rate  $C_w - B_w$  is divided by the measured neutron flux  $\Phi$  of n\_TOF-EAR1 [15]; and the efficiency which, by construction of the TED, is given by  $\varepsilon = S_n + E_n$ . Two extra correction factors are applied:  $f_c$  is a factor that corrects for the counts lost below the amplitude threshold, the multiple detection of photons and the presence of conversion electrons; and  $f_{SRM}$  is

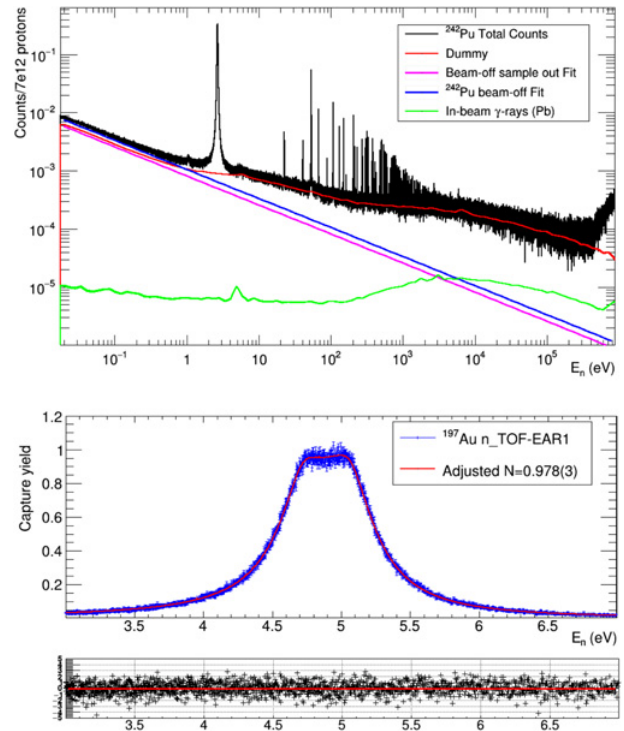


**Figure 1.** Top: measured counting rates per pulse as a function of the incident neutron energy: Total counts and background components. Bottom: SAMMY fit of the capture yield at the Au saturated resonance to extract the normalization factor  $f_{SRM}$ . The residuals of the fit are shown below.

the absolute normalization factor obtained through the *Saturated Resonance Method* applied to the first resonance of  $^{197}\text{Au}$ , shown in Fig. 1 (right panel).

#### 4. Preliminary resonance analysis (up to 2.4 keV)

Once the normalized capture yield is obtained, the resonance analysis has been completed using the SAMMY code [16], which allows fitting experimental ToF data to analytical cross sections generated using the Reich-Moore approximation to the R-matrix theory, and takes into account experimental effects such as the Doppler broadening, the Resolution Function and the small residual background. In our preliminary analysis, we have identified 126 s-wave resonances between 1 eV and 2.4 keV. Figure 2 shows two different energy ranges of the n\_TOF capture yield fitted with SAMMY compared to the ENDF-VII [17] and JEFF-3.2 [18] cross sections. In this figure one can appreciate the accumulated counting statistics and the good energy resolution in our data below 1 keV, which allows extracting individual resonance parameters with high accuracy. In addition, 7 resonances, such as the one at 14 eV present in the JEFF-3.2, can be rejected according to our data, illustrating that the input of these evaluations may contain resonances of other isotopes. Last, many new resonances will be added to the evaluations, especially in the high energy limit of the Resolved Resonance Region, which has been extended beyond the current limit in JEFF-3.2 and up to 2.4 keV. This is illustrated in the right panel of Fig. 2. The statistical analysis of the individual resonance parameters

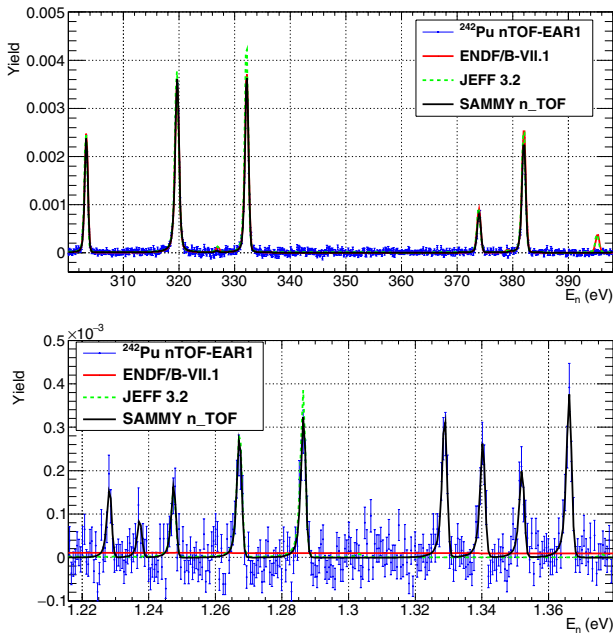


**Figure 2.** Top: capture yield fitted with SAMMY around 300 eV compared to the current evaluations, showing the good level of statistics and energy resolution, and one example of a missing resonance. Bottom: some new resonances are found below 1.3 keV and the RRR is extended above this current energy limit and up to 2.4 keV.

leads to preliminary average resonance parameters. The average level spacing is  $D_0 = 14.8 \pm 0.7$  eV, which is in good agreement with the value of 15.3 eV provided by JEFF-3.2, smaller than the 16.8 eV suggested by Reich et al. [19] and 10% larger than the value given by Mughabghab (ENDF-VII.1) and RIPL [20]. The extracted value for the average radiative width  $\langle \Gamma_\gamma \rangle = 24 \pm 3$  meV is in agreement with all the values in the literature. Finally, the neutron strength function  $S_0 = (0.89 \pm 0.12) \cdot 10^{-4}$  follows the value suggested by Reich et al, which pointed out that the evaluations could be overestimating this parameter by 10%.

## 5. Outlook and complementary measurements

The ToF measurement has successfully taken place at n\_TOF-EAR1 using 95 mg of 99% pure  $^{242}\text{Pu}$  electrodeposited on 7 thin aluminum backings. Preliminary results of the capture yield, resonance analysis and average resonance parameters up to 2.4 keV have been presented. The analysis of the URR, where the background dominates over the capture signals, is ongoing. The ToF measurement will be complemented soon with a thermal capture cross section measurement at the Budapest Research Reactor

(KFKI) [21] combining Activation and Prompt Gamma Analysis. The cross section in the URR region that will be obtained from the n\_TOF data will be complemented with a measurement of the Maxwellian Averaged Cross Section (MACS) at 30 keV using the new neutron line HISPANOS-CNA [22] in Sevilla by means of the activation technique.

This measurement has received funding from the EC FP7 Programme under the projects NEUTANDALUS (Grant No. 334315) and CHANDA (Grant No. 605203), and the Spanish Ministry of Economy and Competitiveness projects FPA2013-45083-P and FPA2014-53290-C2-2-P.

## References

- [1] N. Colonna et al, Energy Environ. Sci. **3**, 1910–1917 (2010)
- [2] *Status and advances in Mox fuel technology* IAEA Technical Reports Series **415** (2003)
- [3] J. Lereendegui-Marco et al., EPJ Web of Conferences **111**, 02005 (2016)
- [4] *NEA High Request Priority List* <http://www.nea.fr/dbdata/hpr1/>
- [5] C. Guerrero, E. Mendoza et al., CERN-INTC-2013-027 (INTC-P-387) (2013)
- [6] C. Guerrero et al., Eur. Phys. J. A **49**, 27 (2013)
- [7] C. Weiss et al., Nucl. Instrum. and Meth. A **799**, 90–98 (2015)
- [8] R. Plag et al., Nucl. Instrum. and Meth. A **496**, 425–436 (2003)
- [9] C. Guerrero et al., Nucl. Instrum. Methods A **608**, 424 (2009)
- [10] CHANDA. FP7-EURATOM-FISSION, EC
- [11] S. Lo Meo et al., Eur. Phys. J. A **51**, 160 (2015)
- [12] R.L. Macklin, J.H. Gibbons, Phys. Rev. **159**, 1007 (1967)
- [13] U. Abbondanno et al., Nucl. Instrum. and Meth. A **521**, 454–467 (2004)
- [14] S. Agostinelli et al., Nucl. Instrum. Methods A **506**, 250 (2003)
- [15] M. Barbagallo et al., (The n\_TOF Collaboration), EPJ A **49**, 156 (2013)
- [16] N.M. Larson, ORNL/TM-9179/R8, ORNL, Oak Ridge, TN, USA (2008)
- [17] M.B. Chadwick et al. ENDF/B-VII.1, Nucl. Data Sheets **112**, 2887 (2011)
- [18] The JEFF-3.1.1 Nuclear Data Library, JEFF Report **22**, OECD/NEA Data Bank (2009)
- [19] Reich et al., Nucl. Sci. Eng. **162**, 178–191 (2009)
- [20] R. Capote et al., Nucl. Data Sheets **110**(12), 3107–3214 (2009)
- [21] T. Belgia, Physics Procedia **31**, 99–109 (2012)
- [22] J. Praena et al., Nucl. Instrum. Meth. A **727**, 1–6 (2013)